Clinical and Experimental Pharmacology and Physiology (2001) **28**, 89–94

Proceedings of the Australian Physiological and Pharmacological Society Symposium: Ion Channels

PREDICTING CHANNEL FUNCTION FROM CHANNEL STRUCTURE USING BROWNIAN DYNAMICS SIMULATIONS

Shin-Ho Chung* and Serdar Kuyucak†

**Protein Dynamics Unit, Department of Chemistry and †Department of Theoretical Physics, Research School of Physical Sciences, Australian National University, Canberra, Australian Capital Territory, Australia*

SUMMARY

1. The transport process of ions across the potassium channel is studied using computer simulations. The shape of the model channel corresponds closely to that deduced from crystallography.

2. We first give an intuitive account of how the motion of ions experiencing an applied electric force and interacting with a dielectric boundary and charge residues on the channel wall can be simulated accurately by using a powerful supercomputer.

3. We then show how some of the salient features of ion channels can be deduced by following the positions of ions at each discrete step over many millions of time steps.

Key words: Brownian dynamics, computer simulations, ion channel, KcsA channel, permeation theory, potassium channel.

INTRODUCTION

There are three prerequisites for constructing a theoretical model of biological ion channels. First, because electric forces play a key role in the movement of ions across the membrane, their correct treatment is very important in modelling ion channels. The forces acting on an ion can be deduced by solving Poisson's equation, but solutions to this equation are difficult for arbitrary channel boundaries separated by the water–protein interface. In the past, studies of the permeation of ions across the transmembrane conduit have been performed almost exclusively in cylindrical geometry, reducing the transport problem to one dimension. The relevance of these studies to real biological channels remains doubtful.

Second, any proposed theoretical model has to be formulated such that it can be validated or refuted experimentally. Thus, a model ion channel should be capable of predicting the magnitude of currents flowing under various conditions. Microscopic simulations in which the motion of individual ions are traced must be performed for periods long enough to measure conductance. Even with the most advanced supercomputer currently available, this requirement has been difficult to meet.

Third, the general shape and dimensions of the channel and the positions and types of various polar groups must be known before one can attempt to build a plausible theoretical model. Until recently, this information has not been available. Towards the aim of building such an accurate theoretical model of ion channels, we have devised an iterative, numerical method of computing electric field at any point in two different dielectric media separated by an arbitrary boundary, for which Poisson's equation cannot be solved analytically.[1] Then, we have devised a method of reducing the amount of computational effort involved in simulating a system of charged particles interacting with a protein wall. Instead of computing force acting on an ion at each position and each time step, we precalculate the values of the electric field for a grid of positions and store them in a set of look-up tables. Using a multidimensional interpolation method, the force experienced by an ion at any position can be deduced from the information stored in the look-up tables.[2] Using this method, we are able to measure the current flowing across a model channel. Recently, the potassium channel from soil bacterium has been crystallized and its crystallographic structure was deduced.[3] Using this newly unveiled structural information and using our own preliminary work, we have made several predictions about the properties of this potassium channel.

METHODS

Until recently, models of ion transport in membrane channels have been dominated by two competing approaches based on reaction rate and continuum theories.[4] In the first approach, also known as Eyring rate theory, the diffusion of ions is modelled as a hopping process. That is, ions move by jumping from site to site, the probability of a hop being determined by the energy difference between the sites and the available thermal energy. While the reaction rate theory provides an intuitive picture for ion permeation in a multi-ion channel, it has no structural basis and, clearly, is not suitable for studying the structure–function relationship.

The continuum theory is based on the solution of two coupled differential equations, the Nernst–Planck equation for the electrodiffusion of ions and Poisson's equation for the mean electric potential; hence, it is dubbed the Poisson–Nernst–Planck (PNP) equation. In this case, the channel structure is included in the calculations and does have an impact on the channel conductance, so the above criticism for the reaction rate theory does not apply.

Correspondence: Shin-Ho Chung, Protein Dynamics Unit, Department of Chemistry, Australian National University, Canberra, ACT 0200, Australia. Email: Shin-Ho.Chung@anu.edu.au

Presented at the Australian Physiological and Pharmacological Society Symposium Ion Channels, September 1999. The papers in these proceedings have been peer reviewed.

Received 15 June 2000; accepted 1 August 2000.

However, comparisons of its predictions with those of Brownian dynamics simulations have indicated that the mean field approximation in PNP theory, that is, the concept of an average potential acting on an average ion density, completely fails in narrow channels with radii less than a Debye length (8 Å for a 150 mmol/L solution). This leads to an overestimation of ionic shielding effects in PNP, so much so that interaction of ions with the dielectric channel boundary is completely neglected. Another shortcoming of PNP is the absence of ion–ion interactions, which are crucial in explaining ion permeation in multi-ion channels, such as potassium and calcium channels. Thus, PNP fails to take into account important structural and dynamic factors in modelling of channels and, hence, cannot be used in predicting channel function from its structure.

The necessity of treating ions as particles leaves molecular and Brownian dynamics (BD) as the only physical theories that allow realistic studies of structure–function relationships in channels. In molecular dynamics, the motion of all the atoms in the system (water, ions and protein forming the channel) are followed using Newton's equation of motion. The force on each atom in the system due to all other atoms is calculated at a given time step and used to determine the new position and velocity of that atom in the next time step. This procedure is repeated until a statistically significant sample of ion trajectories is obtained. While this is conceptually a very simple theory, in practice it is very demanding on computational resources. For example, computation of channel conductance using molecular dynamics is beyond the capabilities of current supercomputers.

In BD, only the motion of ions is simulated, which considerably reduces the computation time, allowing calculation of conductance. Here, a channel is treated as a rigid structure, which can be taken from crystallography if available. The effect of water molecules around an ion is represented by an average frictional force and a random fluctuating force. These two forces can be incorporated into Newton's equation and the resulting stochastic differential equation is known as the Langevin equation. The frictional and random forces act on ions locally as one-body forces and, hence, their handling in BD is quite easy. The systematic forces in the Langevin equation comprise ion–ion and ion–channel interactions. The former is a simple Coulomb interaction modified at short ranges to take into account repulsive forces due to electron clouds of ions and hydration forces. This involves two-body forces and is again relatively simple to implement in BD. In contrast, the ion–channel interaction requires solution of Poisson's equation with relatively complicated boundaries, which can only be performed numerically. Using iterative numerical methods, one can determine the electric forces acting on ions given their positions and channel boundaries. The computational effort required for such a solution is relatively small. However, the fact that ions move to new positions after each time step means that this procedure has to be repeated millions of times during a simulation period. This, too, is time consuming for practical purposes; for example, calculation of conductance for a typical channel would take approximately 1 year on a supercomputer. We have circumvented this computational bottle-neck by introducing look-up tables. The electric field and potential due to one- and two-ion configurations are precalculated at a number of grid points and stored in a set of tables. During simulations, the potential and field at desired points are reconstructed by interpolating between the table entries and using the superposition principle.

We use $\epsilon = 60$ for the dielectric constant of water inside the channel. This choice is dictated by the fact that for lower values of ϵ, the channel ceases to conduct. To simplify the solution of Poisson's equation, the same value $\epsilon = 60$ is used in both the channel and reservoirs. The difference in the Born energies between $\epsilon = 80$ for bulk and $\epsilon = 60$ for channel configurations is included as an energy barrier of height 0.6 kT at both channel entrances.

We solve the Langevin equation using the BD algorithm devised by van Gunsteren and Berendsen,[5] which consists of the following computational steps:

1. Compute the electric force acting on each ion at time t_n and calculate its derivative.
2. Compute a net stochastic force impinging on each ion over a time period of Δt from a sampled value.
3. Determine the position of each ion at time $t_n + \Delta t$ and its velocity at time t_n by using the values of force and its derivative.
4. Repeat the above steps for the desired simulation period.

To simulate the short-range forces more accurately, we use a multiple time-step algorithm in our BD code. A shorter time step of 2 fs is used in the mouth regions of the channel where the Born barrier is active and in the narrow regions where ion–channel interaction is expected to contribute significantly. A long time step of 100 fs is used elsewhere. Specifically, there are two short time-step bands, $-25 < z < -15$ and $7.5 < z < 25$, comprising both entrances and the selectivity filter. If an ion is in one of these bands at the beginning of a 100 fs period, it is simulated by 50 short steps instead of one long step; so, synchronization between the ions is maintained. Long-range forces are calculated normally at the start of the 100 fs period and are assumed to be constant throughout. The ion–ion interactions are normally treated using the long time steps, except when both ions are in one of the above bands.

To mimic the intracellular and extracellular spaces, a cylindrical reservoir with a radius of 30 Å and a variable height is connected to each end of the channel. The number of ions in each reservoir is fixed for convenience (13 of each species, unless otherwise stated) and its height is adjusted to obtain a desired ionic concentration. Simulations under various conditions, each lasting for one million time steps (0.1 μs), are repeated numerous times. Initially, a fixed number of ions is assigned random positions in the reservoirs with velocities also assigned randomly according to the Boltzmann distribution. For successive simulations, the final positions and velocities of the ions in the previous simulation are used as initial positions and velocities in the next trial. The current is determined by the number of ions traversing the channel during the simulation period. To maintain the specified concentrations in the reservoirs, a stochastic boundary is applied: when an ion crosses the channel, say from left to right, an ion of the same species is transplanted from the right reservoir to the left. For this purpose, the ion on the furthermost right-hand side is chosen and it is placed in the far left-hand side of the left reservoir, making sure that it does not overlap with another ion. The stochastic boundary trigger points, located at either pore entrance, are checked at each time step of the simulation.

The BD program is written in Fortran, vectorized and executed on a supercomputer (Fujitsu VPP-300). The time to complete the simulations depends on how often ions enter the short time-step regions. With 48 ions in the system, the central processing unit time needed to complete a simulation period of 1.0 μs (10 million time steps) is roughly 30 h.

Throughout, we quote energy in room temperature units (kT) and dipole moments in Coulomb-meter (Cm). We note $1\,\mathrm{kT} = 4.11 \times 10^{-21}\,\mathrm{J}$ or 0.592 kcal/mol and $1\,\mathrm{Debye} = 3.33 \times 10^{-30}\,\mathrm{Cm}$. The following physical constants were used in our calculations (note that the friction coefficient is related to the diffusion coefficient via the Einstein relation $D = kT/m\gamma$):

masses:

$$m_K = 6.5 \times 10^{-26}\,\mathrm{kg},\ m_{Cl} = 5.9 \times 10^{-26}\,\mathrm{kg}$$

diffusion coefficients:

$$D_K = 1.96 \times 10^{-9}\,\mathrm{m^2/s},\ D_{Cl} = 2.03 \times 10^{-9}\,\mathrm{m^2/s}$$

ion radii:

$$R_K = 1.33\,\text{Å},\ R_{Cl} = 1.81\,\text{Å}$$

room temperature:

$$T = 298\,\mathrm{K}$$

RESULTS AND DISCUSSION

The transverse section of a model channel, shown in Fig. 1, is generated by rotating the two curves around the symmetry z-axis by 180°. The channel is 50 Å long, with a narrow selectivity filter of radius 1.5 Å and length 12 Å. The selectivity filter extends towards the extracellular space, whereas the wider pore, whose radius tapers off gradually, extends inward, towards the intracellular space. The radius at the entrance of the channel from the intracellular space is 3 Å. To render the channel permeable to ions, we place sets of dipoles in the protein wall with four-fold symmetry around the z-axis. First, four rings of four carbonyl groups are placed along the selectivity

filter (filled circles in Fig. 1), such that the negative pole of each carbonyl groups is positioned 1 Å from the boundary and the positive pole 1.2 Å away from the negative pole. Second, four helix macrodipoles (open circles in Fig. 1), with their N-terminals pointing at the oval chamber near the middle of the channel, are placed 90° apart. Third, at each entrance of the channel, four mouth dipoles (filled diamonds in Fig. 1), 5 Å in length, are placed. The strength of each of these three sets of dipoles is optimized so that the channel conductance is largest.

The conductance of channels is one of the most important, experimentally measurable features that characterizes a channel. To deduce the conductance of the model potassium channel with BD,

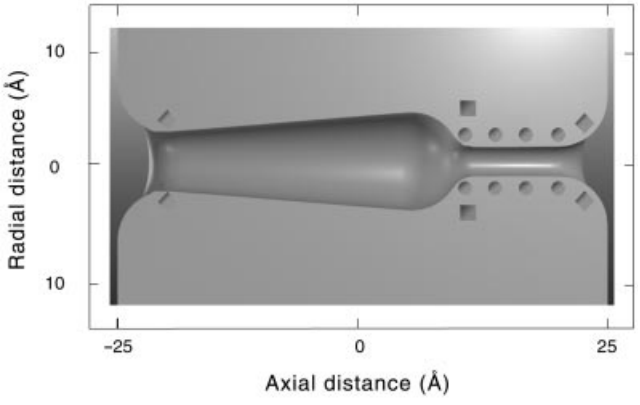

Fig. 1 Model potassium channel. A transverse section of the model channel with the positions of various dipole groups is illustrated. Eight of the 16 carbonyl oxygen atoms, two N-terminals of the four helix dipoles and two of the four mouth dipoles at each entrance are indicated as, respectively, filled circles, open circles and filled diamonds. The strength of these three dipole groups we used are, in units of 10^{-30} Coulomb-meter (Cm), 7.2, 96.2 and 30, respectively.

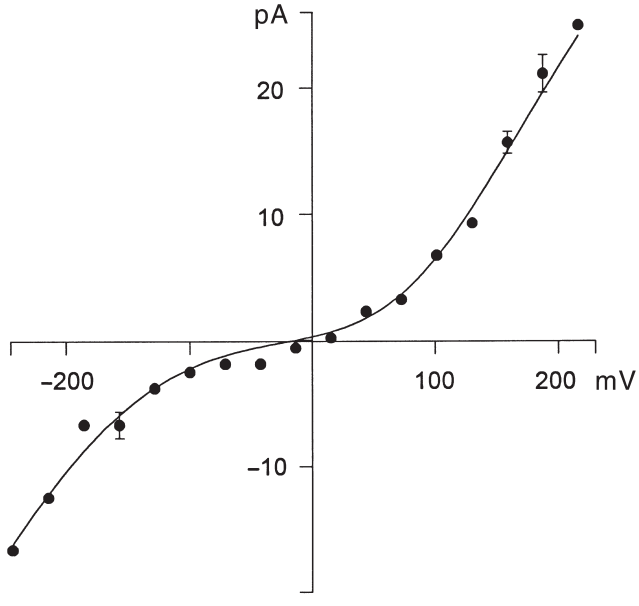

Fig. 2 The current–voltage relationship with symmetrical solutions. The current measured at various applied potentials is obtained with symmetrical solutions of 300 mmol/L in both reservoirs. Each point is derived from a simulation period of 0.5 μs. The error bar accompanying a data point in this and subsequent figures is 1 SEM. $\epsilon = 60$.

the simulation period needs to be sufficiently long that reliable statistics for currents flowing across the channel can be collected. Each point in Fig. 2 is derived from a simulation period of 0.5 μs, or 5 000 000 time steps with an ionic concentration of 300 mmol/L. The current–voltage relationship reveals two distinct features. First, at any given applied potential, the outward current is larger than the inward current. The outward current at 100 mV is 6.7 ± 1.2 pA. Because the current begins to saturate with increasing ionic concentration (see later), the conductance at 150 mmol/L K^+ will be slightly larger than 33 pS. This value is close to the experimentally determined single channel conductance from the *Streptomyces lividans* K^+ channel.[6,7] Second, the current–voltage relationship is ohmic for moderate applied potential, as is the case with many biological channels, but it deviates from the linear Ohm's law as the applied potential increases. Whenever there is an energy barrier in the channel that ions traversing across it have to surmount, a curvature in the current–voltage relationship is expected to be observed. The solid line fitted through the data points is calculated from a theoretical current–voltage relationship that takes into account such an energy barrier. Intuitively, an energy barrier is most effective when the driving force is small and it will be less of an impediment for ions when the driving force is large (see Chung *et al*.[8]). There are some experimental indications for such a deviation of the current–voltage curve from Ohm's law.[9] It will be of theoretical interest to pursue this question further in future patch-clamp experiments where the applied voltage is pushed beyond the usual range of ±100 mV. If such deviations do occur, it should be possible to deduce the height of the energy barrier presented to permeating ions.

The current–voltage relationship obtained with asymmetrical solutions in the two reservoirs is shown in Fig. 3a. The ionic concentrations inside and outside are 500 and 100 mmol/L, respectively. As expected, the asymmetry between the inward and outward currents is accentuated. The zero current of the current–voltage relationship appears to be somewhere between –25 and –50 mV. To ascertain how closely the measured reversal potentials match those predicted by the Nernst equation, we estimate currents flowing across the channel with two different ionic concentrations in the reservoirs and under various applied potentials. The concentration of K^+ in the extracellular and intracellular aspects of the channel are computed from the average number of ions in the reservoirs throughout the simulation periods. The measured ionic concentrations in the left and right reservoirs in one series of simulations are 71.5 and 482.0 mmol/L and, in another series of simulations, are 176.2 and 385.3 mmol/L. Figure 3b shows the currents flowing across the channel at various applied potentials. Because the net current for these driving forces is small, the total simulation period of 3 μs is used to derive each data point. The reversal potential for each asymmetrical solution is estimated by fitting a polynomial curve through the data points (solid lines in Fig. 3b). There are small but consistent discrepancies between the reversal potentials deduced from simulations and those predicted from the Nernst equation (indicated with open downward arrows). The zero currents occur at –45 and –17 mV when the concentration ratios in the two reservoirs are 6.7 : 1 and 2.2 : 1, respectively. The predicted reversal potentials are –48.1 and –19.7 mV. These discrepancies between the predicted and measured zero currents disappear if we take the activity coefficients of KCl at the measured ionic concentrations into account, as indicated by the filled arrows in Fig. 3b. The values of activity coefficients used for 71.5, 176.2, 386.3 and 482.0 mmol/L are 0.79,

0.73, 0.67 and 0.63, respectively. From the number of such current–voltage relationships obtained with asymmetrical solutions, we conclude that the zero current occurs at a potential predicted by the Nernst equation, provided the activity of the solution is taken into account.

It has been known for some time that the potassium channel is normally occupied by several ions. It is of interest to deduce where in the channel ions dwell predominantly. To compute the average number of ions inside the channel, we divide the channel into 32 thin sections, as indicated in the inset of Fig. 4, and compute the time averages of potassium ions in each section. For this series of calculations, we use ionic concentrations of 500 and 100 mmol/L in the reservoirs representing, respectively, the intracellular and extracellular spaces. When a potential of 200 mV is applied so as to produce an inward current, two ions, on average, tend to reside in the channel. The preferred positions where ions dwell are in the selectivity filter at $z = 9.4$ and 17.2 Å (Fig. 4a). The preferred positions of the ions in the channel are shifted when the direction of the current is reversed by making the inside positive with respect to the outside. Under these conditions, again two ions mainly linger in the channel but the preferred positions where ions dwell are shifted. Instead of two, there are now three peaks in the histogram (Fig. 4b), the peaks centred around 9.4, 14.1 and 23.4 Å. We note here that, although the histogram shows three distinct peaks near the selectivity filter, there are, on average, 1.5 ions in this region, as can be deduced by summing the heights of the bars. A similar sum for the peak near the intracellular entrance gives 0.7 ions; that is, an ion is present there 70% of the time. It must be emphasized that ions in the channel are not firmly 'bound' at two or three fixed positions; rather, they undergo perpetual thermal motions. The time average of the positions reveals the relative probabilities of finding ions along the channel axis. Comparison of the two histograms reveals that these preferred sites shift as the direction of the applied potential is reversed.

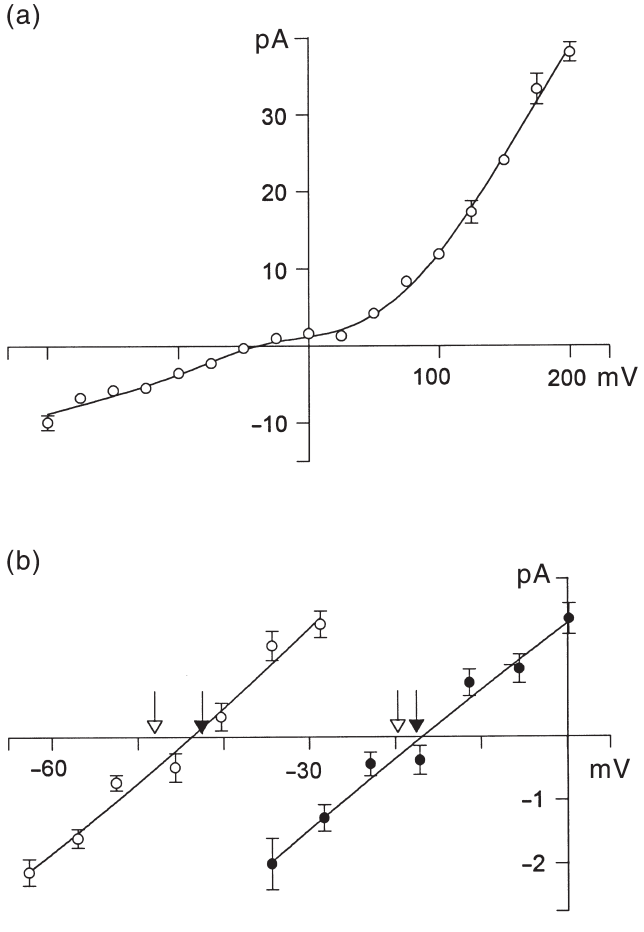

Fig. 3 The current–voltage relationships with asymmetrical solutions. The current measured at various applied potentials is obtained with asymmetrical solutions. (a) The concentrations in the reservoir representing the intracellular and extracellular space are 500 and 100 mmol/L, respectively. $\epsilon = 60$. (b) The measured concentrations in the intracellular and extracellular reservoirs are 482.0 and 71.5 mmol/L (○), respectively, and 385.3 and 176.2 mmol/L (●), respectively. The open downward arrows indicate the reversal potential calculated from the Nernst equation. The predicted Nernst potentials taking the activity coefficient into account are indicated with filled downward arrows. $\epsilon = 80$.

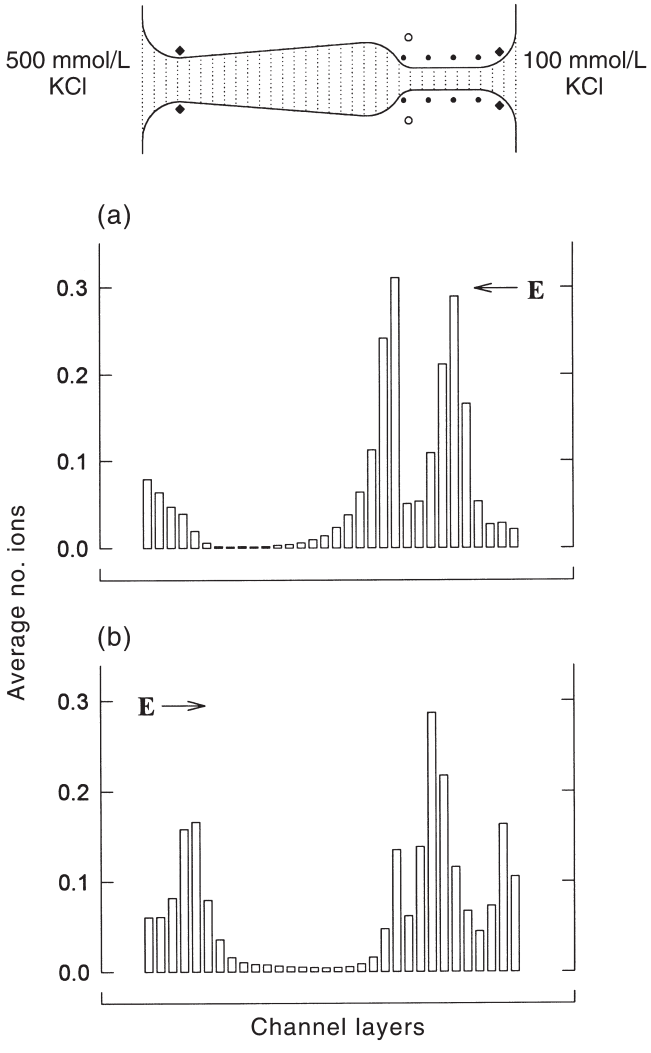

Fig. 4 Concentrations of potassium ions in the channel. The channel is divided into 32 sections, as indicated in the inset, and the probability of ions present in each section over a simulation period of 0.5 μs is tabulated (bars). The ionic concentrations in the intracellular and extracellular reservoirs are 500 and 100 mmol/L, respectively. The applied potential in (a) is +200 mV, inside positive with respect to outside, whereas the direction of the potential is reversed in (b). E, applied electric field.

Experimentally, a current across a biological ion channel generally increases with increasing ionic concentration and then saturates with a further increase in concentration. Saturation of the channel current occurs when there is a rate-limiting permeation process that is independent of ionic concentrations. For example, an ion arriving near the entrance of the intracellular aspect of the channel will be detained there for a period of time if, before traversing towards the selectivity filter, it needs to gain a sufficient kinetic energy to climb over an energy barrier. As shown in Fig. 5, the magnitude of current across the channel plotted against the concentrations of potassium ions in the reservoirs has the same shape as those observed experimentally.[10,11] The two curves in Fig. 5 are the outward and inward currents using an applied potential of 200 mV. The fitted lines through the data points are calculated from the Michaelis–Menten equation. The half-saturation values determined from the data are 151 ± 11 mmol/L for the outward current and 127 ± 11 mmol/L for the inward current. These values are slightly higher than the experimentally determined value for a potassium channel from sarcoplasmic reticulum by Coronado *et al*.[10]

The conduction of ions across the potassium channel is critically dependent on the strength of dipoles lining the channel entrance from the intracellular space. In Fig. 6, we plot the magnitude of the outward current as a function of the strength of each mouth dipole. The conductance increases rapidly as the moment of each dipole is increased from 10×10^{-30} Cm. The current begins to decline when the moment is further increased to 60×10^{-30} Cm. The current flowing across the channel is largest when the charge on each of the four dipoles is 0.6×10^{-19} C and a small increase or decrease in the strength of dipoles causes the channel to close. This fact leads us to speculate that the opening and closing of the potassium need not be steric. In theory, at least, the transition between the closed and open states may be achieved by changing the strength of dipoles surrounding the channel entrance.

For example, the channel in the closed state may have the mouth dipoles orientated parallel to the rim of the entrance wall so that their net moment viewed from the central axis will be zero, whereas in its open state the dipoles may orientate perpendicular to the channel rim. The channel may be in a conductance substate when the dipoles are not optimally orientated. These possibilities are schematically illustrated in Fig. 6b. Alternatively, the channel in the closed state may possess mouth dipoles that are much larger than those required for optimal conduction. In such a case, the channel will begin to conduct when the effective charges on the dipoles are reduced by protonation or otherwise (Fig. 6c).

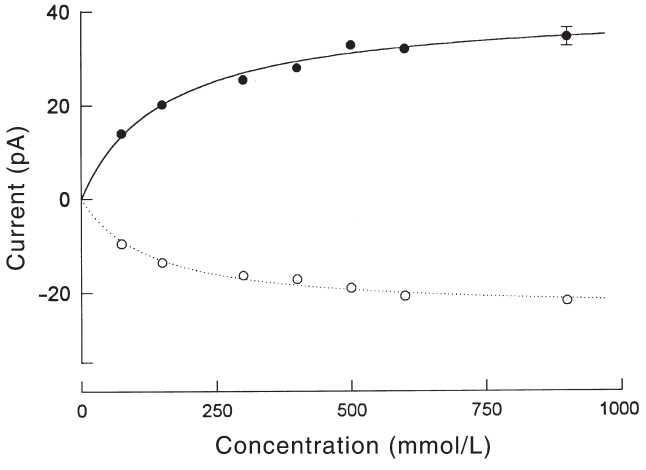

Fig. 5 The conductance–concentration curves for the outward (●) and inward (○) currents. An applied potential of 200 mV and symmetrical solutions of varying concentrations in the two reservoirs are used. The lines fitted through the data points are calculated with the Michaelis–Menten equation. Each point is derived from a simulation period of 1 μs.

CONCLUSIONS

We have used the recently unveiled structural information about the potassium channel in BD studies to understand its conduction

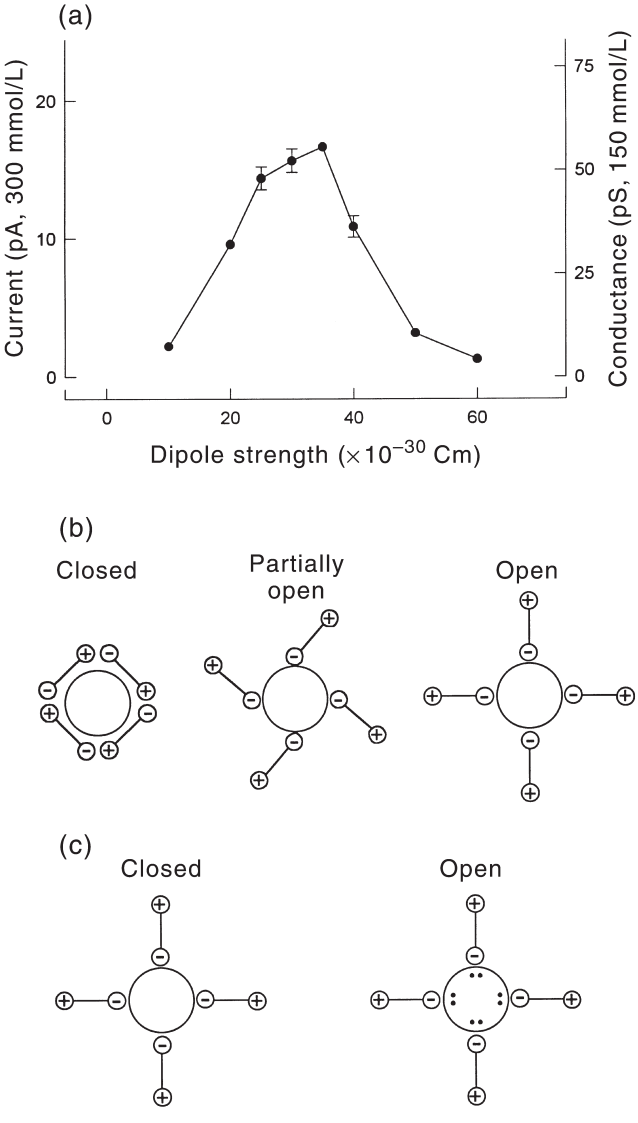

Fig. 6 Changes in channel conductance with the strength of mouth dipoles. (a) The strength of each mouth dipole is changed systematically while keeping the moments of each carbonyl group and helix dipole constant at 7.2 and 96.3×10^{-30} Cm. (b) One possible way the channel may change from the fully closed to partially and fully open states is illustrated schematically. The channel entrance is viewed from the intracellular side. The orientation of dipoles to the optimal angles to suboptimal angles may cause the channel to close. (c) Alternatively, conduction may take place only when the effective strength of mouth dipoles is reduced by protons in the solution, indicated here by black dots.

properties. We show that approximately two ions are attracted to the deep well created by a set of dipoles on the channel wall. These ions most commonly dwell near the equilibrium positions of two ions in the potential well. A third ion entering the channel triggers the motion of the resident ions via the ion–ion repulsive force, so initiating a conduction event. The channel conductance determined from BD simulations agrees closely with that determined experimentally. The current–voltage relationship obtained with symmetrical solutions is linear when the applied potential is less than 100 mV, but deviates from Ohm's law at a higher applied potential. The reversal potentials obtained with asymmetrical solutions are in agreement with those predicted by the Nernst equation. The conductance exhibits the saturation property observed experimentally. Finally, we demonstrate that, for conduction to take place, the strength of four dipoles guarding the channel entrance facing the extracellular space must be optimum. An increase or decrease of the dipole strength from this optimal value effectively closes the channel. We postulate that the opening or closing of the potassium channel may be governed by protonation of these mouth dipoles or a small rotation of their orientation.

REFERENCES

1. Hoyles M, Kuyucak S, Chung SH. Solutions of Poisson's equation in channel-like geometries. *Comput. Phys. Commun.* 1998; **115**: 45–68.
2. Hoyles M, Kuyucak S, Chung SH. Computer simulation of ion conductance in membrane channels. *Phys. Rev. E* 1998; **58**: 3654–61.
3. Doyle DA, Cabral JM, Pfuetzner RA *et al.* The structure of the potassium channel: Molecular basis of K^+ conduction and selectivity. *Science* 1998; **280**: 69–77.
4. Hille B. *Ionic Channels of Excitable Membranes*, 2nd edn. Sinauer Associates, Suntherland, MA. 1992.
5. van Gunsteren WF, Berendsen HJC. Algorithm for Brownian dynamics. *Mol. Phys.* 1982; **45**: 637–47.
6. Schrempf H, Schmidt O, Kummerlen R *et al.* A prokaryotic potassium ion channels with two predicted transmembrane segment from *Streptomyces lividans*. *EMBO J.* 1995; **14**: 5170–8.
7. Heginbotham L, LeMasurier M, Kolmakova-Partensky L, Miller C. Single *Streptomyces lividans* K^+ channels. Functional asymmetries and sidedness of proton activation. *J. Gen. Physiol.* 1999; **114**: 551–9.
8. Chung SH, Hoyles M, Allen T, Kuyucak S. Study of ionic currents across a model membrane channel using Brownian dynamics. *Biophys. J.* 1998; **75**: 793–809.
9. Tyerman SD, Terry BR, Findlay GP. Multiple conductances in the large K^+ channel from *Chara corallina* shown by a transient analysis method. *Biophys. J.* 1992; **61**: 736–49.
10. Coronado R, Rosenberg RL, Miller C. Ionic selectivity, saturation, and block in a K^+-selective channel from sarcoplasmic reticulum. *J. Gen. Physiol.* 1980; **76**: 425–46.
11. Rae JL, Levis RA, Eisenberg RS. Ionic channels in ocular epithelia. In: Narhashi T (ed.). *Ion Channels*, Vol. 1. Plenum Press, New York. 1988; 283–327.